

Collisional excitation of water by hydrogen atoms

F. Daniel^{1*}, A. Faure¹, P. J. Dagdighian², M.-L. Dubernet^{3,4}, F. Lique⁵, G. Pineau des forêts^{6,7}

¹ Univ. Grenoble Alpes / CNRS, IPAG, F-38000 Grenoble, France

² Department of Chemistry, The Johns Hopkins University, Baltimore, Maryland 21218-2685, USA

³ Université Pierre et Marie Curie, LPMMA, UMR CNRS 7092, 75252 Paris, France

⁴ Observatoire de Paris, LUTH, UMR CNRS 8102, 92195 Meudon, France

⁵ LOMC-UMR 6294, CNRS-Université du Havre, 25 rue Philippe Lebon, BP 540 76058 Le Havre France

⁶ LERMA, UMR 8112, CNRS, Observatoire de Paris, ENS, UPMC, UCP, 61 avenue de l'Observatoire, F-75014 Paris

⁷ IAS, UMR 8617, CNRS, Bâtiment 121, Université Paris Sud 11, 91405, Orsay, France

Accepted XXX. Received XXX; in original form XXX

ABSTRACT

We present quantum dynamical calculations that describe the rotational excitation of H₂O due to collisions with H atoms. We used a recent, high accuracy potential energy surface, and solved the collisional dynamics with the close-coupling formalism, for total energies up to 12 000 cm⁻¹. From these calculations, we obtained collisional rate coefficients for the first 45 energy levels of both ortho- and para-H₂O and for temperatures in the range T = 5–1500 K. These rate coefficients are subsequently compared to the values previously published for the H₂O / He and H₂O / H₂ collisional systems. It is shown that no simple relation exists between the three systems and that specific calculations are thus mandatory.

Key words: molecular data – molecular processes – scattering

1 INTRODUCTION

In astrophysical studies, water is an important molecule which has been observed in many different media, ranging from cold prestellar cores (Caselli et al. 2010, 2012), to warm intermediate and high mass star-forming regions (Cernicharo et al. 1994, 2006), circumstellar envelopes (see e.g. González-Alfonso & Cernicharo 1999; Decin et al. 2010) or extragalactic sources (González-Alfonso et al. 2004). In these media, the emission observed for H₂O is often associated with shocked gas (Cernicharo et al. 1999; Flower & Pineau Des Forêts 2010; Neufeld et al. 2014). An extensive view of the water component in these regions can be found in the reviews by Cernicharo & Crovisier (2005) and by van Dishoeck et al. (2011, 2013).

In order to interpret the H₂O line intensities and infer the physical and chemical properties of the observed regions, the most reliable methodology relies on radiative transfer calculations. Indeed, for most of these objects, the water energy levels are often populated under non-LTE conditions. It is thus necessary to know the H₂O collisional rate coefficients with the relevant collisional partners, namely H₂, He, e⁻ and H. Extensive collisional data sets are now available for the three former colliders (Daniel et al. 2011; Green et al. 1993; Faure et al. 2004; Faure & Josselin 2008). The collision between a H₂O molecule and H atom has been the subject of many studies (see e.g. Jiang et al. 2011; Fu & Zhang 2013).

However, most of these works were only focused on reactive collisions and in the formation of the OH and H₂ molecules. To the best of our knowledge, no quantum state-to-state rate coefficients have been published for the inelastic collisions.

The molecules for which rate coefficients have been obtained with H as a collisional partner are limited. Indeed, in the case of molecules which have been detected in the interstellar medium, the only available calculations consider CO (Chu & Dalgarno 1975; Green & Thaddeus 1976; Balakrishnan et al. 2002; Shepler et al. 2007; Yang et al. 2013), CO⁺ (Andersson et al. 2008), N₂ (Stoeklin & Voronin 2007), H₂ (Forrey et al. 1997; Flower & Roueff 1998; Wrathmall & Flower 2006; Lique et al. 2012) and HD (Flower & Roueff 1999; Roueff & Flower 1999). To date, no data are available for the inelastic rate coefficients of the H₂O / H collisional system. Therefore, these quantities are usually inferred by scaling either the H₂O / He (Nesterenok & Varshalovich 2014, e.g.) or H₂O / H₂ (Flower & Pineau Des Forêts 2010, e.g.) collisional rate coefficients, when needed. In the current study, we provide rate coefficients for the H₂O / H system and comment on the possibility of scaling the rates from other collisional systems to have an estimate of such rates. These collision rates are of particular importance in predicting and interpreting H₂O line emission in shocks propagating in the molecular interstellar medium. Indeed, in J-type shocks with velocities greater than 15–20 km/s, the temperature behind the shock front is sufficient to dissociate molecular hydrogen and there is a large range of temperature (300–2000K) where H₂O and atomic hydrogen coexist and where the cool-

* E-mail: fabien.daniel@obs.ujf-grenoble.fr

ing can be dominated by H₂O line emission (Flower et al. 2003; Flower & Pineau Des Forêts 2010). Finally, in such regions, some water lines may exhibit population inversion. In order to interpret the emission from these masers, it is necessary to describe accurately the rates at which the upper and lower states are populated, which thus depends on the collisional rate coefficients used (Daniel & Cernicharo 2013; Hollenbach et al. 2013).

This article is organized as follows. In Sect. 2, we describe the potential energy surface used in the current work. In Sect. 3, we present the quantum dynamical calculations and in Sect. 4, we discuss the current rate coefficients with respect to other collisional systems involving the water molecule.

2 POTENTIAL ENERGY SURFACE

A high accuracy potential energy surface (PES) for the interaction of H₂O with a hydrogen atom was computed recently by Dagdigian & Alexander (2013). The rigid-rotor approximation was employed with the water geometry kept fixed at its vibrationally averaged geometry. The reactive channel leading to OH + H₂ is thus ignored and the PES is three-dimensional. The rigid-rotor approximation is valid at the temperatures investigated here since the activation energy for the reaction is high (~ 9300 K) and the rate coefficient is only $\sim 2 \times 10^{-13} \text{ cm}^3 \text{ s}^{-1}$ at 1500 K (Baulch et al. 1992). Dagdigian & Alexander (2013) employed restricted coupled cluster calculations with inclusion of single and double excitations, augmented by a perturbational estimate of the connected triple excitations [RCCSD(T)]. A quadruple zeta quality basis set was used, with the addition of mid-bond functions, and a counterpoise correction was applied to correct for basis set superposition error (BSSE). By exploiting symmetry, a total of 3800 nuclear geometries only were computed for atom-molecule separations ranging from 3 to 10 bohr. Full details about the PES and the H₂O–H system can be found in Dagdigian & Alexander (2013).

In order to interface the H₂O–H potential of Dagdigian & Alexander (2013) with the MOLSCAT scattering program (see below), it was necessary to perform a new angular expansion of the PES. Indeed, the coordinates used by Dagdigian & Alexander (2013) to describe the H₂O–H PES (see Fig. 1 of their paper) are different from those required by MOLSCAT for an atom-asymmetric top system. As a result, the 3800 nuclear geometries were converted to the MOLSCAT coordinate system where the z axis is the symmetry axis of water. This conversion corresponds in practice to a single rotation by an angle of 90° about the y axis, which is common to both sets of coordinates. The resulting new spherical coordinates were duplicated in the whole sphere, i.e. $\theta \in [0, 180]^\circ$ and $\phi \in [0, 360]^\circ$, both varied in steps of 10° , for a total of 12 620 nuclear geometries (631 per intermolecular separation).

The H₂O–H PES expressed in the MOLSCAT coordinate system was expanded in spherical harmonics, $Y_{\lambda\mu}(\theta, \phi)$, as in Dagdigian & Alexander (2013) (see their Eq. 13), using a linear least-square fit procedure¹. As in Dagdigian & Alexander (2013), all terms with $\lambda \leq 10$ and $\mu \leq 8$ were included in the expansion, resulting in a total of 35 angular terms. The root mean square residual was found to be lower than 1 cm^{-1} for intermolecular separations R larger than 4 bohr. As an illustrative example, the global

¹ We note that in the MOLSCAT coordinate system, the C_{2v} symmetry of H₂O requires that μ is even, while in the original coordinate system, symmetry restricts the expansion to terms with $\lambda + \mu$ even.

minimum of the PES was found by Dagdigian & Alexander (2013) to have an energy of -61.0 cm^{-1} , at a geometry of $R=6.5$ bohr, $\theta = 120^\circ$, $\phi = 0^\circ$ (in MOLSCAT coordinates). Using our fit, we obtained -61.3 cm^{-1} , in excellent agreement. This latter value can also be compared with the global minima of the PES for the similar systems H₂O–He (-34.9 cm^{-1} at $R=5.9$ bohr, $\theta = 75^\circ$, $\phi = 0^\circ$ Patkowski et al. (2002)) and H₂O–H₂ (-235.1 cm^{-1} at $R=5.8$ bohr, $\theta = 0^\circ$, $\phi = 0^\circ$, Faure et al. (2005); Valiron et al. (2008)). The interaction of water with hydrogen atoms is thus very different from the interactions with He and H₂. We can therefore expect significant differences in the corresponding rotational rate coefficients.

3 COLLISIONAL DYNAMICS

In order to solve the collisional dynamics, we used the MOLSCAT² code. Benchmark calculations were also performed with the HIBRIDON³ code using the original fit of the H₂O–H PES by Dagdigian & Alexander (2013). We tested both codes at a few total energies and the cross sections were found to be essentially similar, within 5%. We performed the calculations in order to provide rate coefficients for the first 45 energy levels of the ortho- and para-H₂O symmetries, i.e. up to $J_{K_a, K_c} = 7_{7,0}$ ($E \sim 1395 \text{ cm}^{-1}$) for o-H₂O and up to $J_{K_a, K_c} = 7_{7,1}$ ($E \sim 1395 \text{ cm}^{-1}$) for p-H₂O. Calculations have been performed up to a total energy of $12\,000 \text{ cm}^{-1}$ and we have used the close-coupling formalism over the whole energy range. This enables to provide converged rate coefficients for the range of temperature $T = 5 - 1500\text{K}$. The parameters of the calculations, i.e. the number of H₂O energy levels, the integration step and the step between two consecutive energies were determined in order to ensure an accuracy better than 5% for the rate coefficients. These parameters are given in Tables 1 and 2. Additionally, we included a cut in energy for the H₂O energy levels, set to $E_{max} = 3000 \text{ cm}^{-1}$ below total energy of 5000 cm^{-1} and $E_{max} = 4000 \text{ cm}^{-1}$ above this threshold.

The water energy levels are described using the effective Hamiltonian of Kyrö (1981), as previously done in our quantum calculations that dealt with the H₂O / H₂ system (Dubernet & Grosjean 2002; Grosjean et al. 2003; Dubernet et al. 2006, 2009; Daniel et al. 2010, 2011). We used the hybrid modified log-derivative Airy propagator of Alexander & Manolopoulos (1987), the change of propagator being set at $20 a_0$. The reduced mass of the collisional system is $\mu = 0.954418234$ amu.

4 RATE COEFFICIENTS

The collisional de-excitation rate coefficients are calculated by averaging the cross sections with a Maxwell–Boltzmann distribution

² J. M. Hutson and S. Green, MOLSCAT computer code, version 14 (1994), distributed by Collaborative Computational Project No. 6 of the Engineering and Physical Sciences Research Council (UK).

³ HIBRIDON is a package of programs for the time-independent quantum treatment of inelastic collisions and photodissociation written by M. H. Alexander, D. E. Manolopoulos, H.-J. Werner, B. Follmeg, Q. Ma, and P. J. Dagdigian, with contributions by P. F. Vohralik, D. Lemoine, G. Corey, R. Gordon, B. Johnson, T. Orlikowski, A. Berning, A. Degli-Esposti, C. Rist, B. Pouilly, G. van der Sanden, M. Yang, F. de Weerd, S. Gregurick, J. Klos and F. Lique. More information and/or a copy of the code can be obtained from the website <http://www2.chem.umd.edu/groups/alexander/hibridon/hib43>.

Table 1. Parameters that govern the convergence of the MOLSCAT calculations: J1max which is the highest value of the rotational quantum number and the parameter STEPS which is inversely proportional to the step of integration. These parameters are given for the two water symmetries as a function of the total energy.

Energy range (cm ⁻¹)	p-H ₂ O		o-H ₂ O	
	J1max	STEPS	J1max	STEPS
< 42	4	20	4	50
42–80	4	10	4	20
80–230	6	10	5	10
230–310	6	10	6	10
310–410	7	10	7	10
410–500	8	10	8	10
500–600	9	10	9	10
600–750	10	10	10	10
750–1000	11	10	11	10
1000–1250	12	10	12	10
1250–1500	13	10	13	10
1500–2000	14	10	14	10
2000–3000	15	10	15	10
3000–5000	16	10	16	10
5000–12000	18	10	18	10

Table 2. Step between the consecutive total energies used to characterize the cross sections.

Energy range (cm ⁻¹)	step in energy (cm ⁻¹)
< 1250	0.1
1250 – 2000	0.5
2000 – 2500	5.0
2500 – 3000	10.0
3000 – 12000	50.0

that describes the distribution of velocity of the molecules in the gas (see e.g. eq. (2) in Dubernet et al. 2006)

$$R_{\beta,\beta'}(T) = \left(\frac{8}{\mu\pi}\right)^{\frac{1}{2}} \frac{1}{(k_B T)^{\frac{3}{2}}} \int_0^{\infty} \sigma_{\beta,\beta'}(E) E e^{-E/k_B T} dE \quad (1)$$

where β and β' are a set of quantum numbers that describe the initial and final states of water, k_B is the boltzmann constant, μ is the reduced mass of the colliding system and E is the kinetic energy. In Table 3, we give the de-excitation rate coefficients for levels up to $J_{K_a,K_c} = 3_{3,0}$, and for temperatures in the range $T = 20$ – 1000 K. The whole set of rate coefficients, with higher temperatures and with a more extended set of molecular levels will be made available through the LAMDA (Schöier et al. 2005) and BASECOL (Dubernet et al. 2013) databases.

In astrophysical applications, it is rather common to need rate coefficients which are not available. Therefore, it is quite usual to infer the rate coefficients of a colliding system from the values calculated for closely related system. The methodology which is generally used, even if its theoretical basis are questionable (Walker et al. 2014), consist in assuming that the cross sections $\sigma_{\beta,\beta'}(E)$ which appear in eq. (1), are similar for both systems. The rate coefficients are then derived by correcting for the change in reduced mass, which lead to the scaling relationships: $R_{\beta,\beta'}^2(T) = \sqrt{\mu_1/\mu_2} \times R_{\beta,\beta'}^1(T)$. As an example, in the current case, we could apply this methodology to infer the H₂O / H rate coefficients from

either the H₂O / He or H₂O / p-H₂ rate coefficients. This would lead to rate coefficients such that $R_{\beta,\beta'}^H \sim 1.8 \times R_{\beta,\beta'}^{He}$ or $R_{\beta,\beta'}^H \sim 1.4 \times R_{\beta,\beta'}^{H_2}$. In table 3, we compare the current H₂O / H rate coefficients with the rate coefficients of the H₂O / He (Yang et al. 2013) and H₂O / p-H₂ (Dubernet et al. 2009) systems, for o-H₂O energy levels up to $J_{K_a,K_c} = 3_{3,0}$ ($E \sim 285$ K). In Fig. 1, we give the ratios of the current o-H₂O / H rate coefficients with the He rate coefficients of Green et al. (1993) and with the H₂ rates of Dubernet et al. (2009), for the first 45 o-H₂O energy levels. In the case of He, we used the rate coefficients from Green et al. (1993) since the most recent calculations by Yang et al. (2013) only consider the first 10 water energy levels. Additionally, as pointed out in the latter study, the impact of the new calculation is modest at high temperatures, the differences being lower than 30% above 200K. At lower temperatures, however, differences of up to a factor 3 can be found between the two sets. Considering the values taken by the ratios, it is obvious that no simple scaling relationship relate the various collisional rate coefficient sets, with differences that span various orders of magnitude. However, we note that the scatter of the ratios tends to decrease when increasing temperature. Moreover, for the largest rates at high temperature, the rate coefficients for the various colliders become similar, within a factor 2. This was expected since at high collision energy the scattering process becomes dominated by kinematics rather than specific features of the PES. Such conclusions were already reached for other collisional systems (see e.g. Roueff & Flower 1999, for the HD molecule). In summary, a dedicated calculation is a pre-requisite to accurately describe the collision with either H₂, He or H, especially at temperatures below ~ 1000 K.

5 CONCLUSIONS

We described quantum dynamical calculations performed at the close-coupling level of theory for the H₂O / H collisional system. As a result, we give collisional rate coefficients for the first 45 energy levels of both ortho- and para-H₂O and for temperatures in the range $T = 5$ – 1500 K. These calculations complete the sets already calculated for the water molecule, for which specific calculations are now available for all the colliders relevant to studies dealing with the interstellar medium, i.e. H₂, He, H and e^- . In particular, we examined the possibility of emulating the H₂O / H rate coefficients by a simple scaling of either the H₂O / He or H₂O / H₂ sets and found that no simple relation enable to relate a set to another.

ACKNOWLEDGMENTS

Most of the computations presented in this paper were performed using the CIMENT infrastructure (<https://ciment.ujf-grenoble.fr>), which is supported by the Rhône-Alpes region (GRANT CPER07_13 CIRA: <http://www.ci-ra.org>). This work has been supported by the Agence Nationale de la Recherche (ANR-HYDRIDES), contract ANR-12-BS05-0011-01 and by the CNRS national program ‘‘Physico-Chimie du Milieu Interstellaire’’.

REFERENCES

- Alexander, M. H., & Manolopoulos, D. E. 1987, J. Chem. Phys., 86, 2044
 Andersson, S., Barinovs, G., & Nyman, G. 2008, ApJ, 678, 1042
 Balakrishnan, N., Yan, M., & Dalgarno, A. 2002, ApJ, 568, 443

Table 3. H₂O / H de-excitation rate coefficients ($R_{\beta\beta'}^H$ in $\text{cm}^3 \text{s}^{-1}$, where the notation $x(y)$ stands for $x 10^y$) as a function of temperature and for H₂O levels up to $J_{Ka,Kc} = 3_{3,0}$. For each temperature, we give the ratio of the current rate coefficients with the He rate coefficients of Yang et al. (2013) (second column), and with the para-H₂ rate coefficients of Dubernet et al. (2009) (third column).

Transition	20K			100K			500K			1000K		
	$R_{\beta\beta'}^H$	H / He	H / H ₂	$R_{\beta\beta'}^H$	H / He	H / H ₂	$R_{\beta\beta'}^H$	H / He	H / H ₂	$R_{\beta\beta'}^H$	H / He	H / H ₂
1 _{1,0} → 1 _{0,1}	9.54(-12)	0.78	0.28	1.88(-11)	0.62	0.46	6.84(-11)	0.85	0.70	1.06(-10)	1.07	0.83
2 _{1,2} → 1 _{0,1}	1.24(-11)	0.68	0.37	1.71(-11)	0.62	0.46	5.24(-11)	0.89	0.75	8.09(-11)	1.11	0.94
2 _{1,2} → 1 _{1,0}	6.34(-13)	0.11	0.04	9.66(-13)	0.14	0.08	3.54(-12)	0.40	0.42	6.39(-12)	0.71	0.86
2 _{2,1} → 1 _{0,1}	8.60(-13)	1.22	0.26	1.86(-12)	0.89	0.40	9.00(-12)	0.73	0.80	1.50(-11)	0.70	0.86
2 _{2,1} → 1 _{1,0}	1.80(-11)	2.07	0.54	2.00(-11)	1.16	0.56	4.90(-11)	1.09	0.79	7.36(-11)	1.27	0.96
2 _{2,1} → 2 _{1,2}	6.32(-12)	0.57	0.34	9.07(-12)	0.53	0.47	2.62(-11)	0.78	0.68	3.91(-11)	0.99	0.80
3 _{0,3} → 1 _{0,1}	7.51(-13)	0.49	0.10	1.48(-12)	0.42	0.19	6.91(-12)	0.57	0.74	1.23(-11)	0.70	1.11
3 _{0,3} → 1 _{1,0}	2.61(-12)	0.51	0.43	3.60(-12)	0.49	0.60	1.09(-11)	0.90	1.15	1.78(-11)	1.19	1.69
3 _{0,3} → 2 _{1,2}	9.32(-12)	0.68	0.27	1.28(-11)	0.61	0.40	3.68(-11)	0.82	0.65	5.56(-11)	1.02	0.81
3 _{0,3} → 2 _{2,1}	1.18(-12)	2.16	0.27	7.44(-13)	0.36	0.32	3.19(-12)	0.30	0.79	7.83(-12)	0.52	1.10
3 _{1,2} → 1 _{0,1}	5.32(-13)	1.68	0.66	5.68(-13)	1.01	0.73	1.34(-12)	1.18	0.96	2.11(-12)	1.36	1.18
3 _{1,2} → 1 _{1,0}	1.02(-12)	1.16	0.28	1.85(-12)	0.87	0.40	9.47(-12)	1.07	1.36	1.74(-11)	1.23	2.10
3 _{1,2} → 2 _{1,2}	1.41(-12)	0.33	0.08	2.97(-12)	0.41	0.18	1.56(-11)	0.63	0.82	2.77(-11)	0.73	1.22
3 _{1,2} → 2 _{2,1}	3.00(-12)	0.69	0.18	3.76(-12)	0.50	0.31	1.47(-11)	0.94	0.91	2.63(-11)	1.30	1.44
3 _{1,2} → 3 _{0,3}	7.80(-12)	0.71	0.37	1.42(-11)	0.71	0.53	5.12(-11)	0.95	0.83	8.15(-11)	1.17	1.00
3 _{2,1} → 1 _{0,1}	1.69(-12)	2.57	2.18	2.34(-12)	1.24	1.91	9.59(-12)	0.93	1.83	1.72(-11)	1.01	1.84
3 _{2,1} → 1 _{1,0}	2.39(-13)	1.49	0.57	2.80(-13)	0.71	0.48	4.63(-13)	0.40	0.38	6.39(-13)	0.42	0.38
3 _{2,1} → 2 _{1,2}	1.17(-11)	3.14	0.84	1.28(-11)	1.58	0.80	3.05(-11)	1.24	1.06	4.76(-11)	1.36	1.30
3 _{2,1} → 2 _{2,1}	1.32(-12)	0.28	0.07	2.77(-12)	0.36	0.13	1.48(-11)	0.78	0.82	2.76(-11)	1.01	1.57
3 _{2,1} → 3 _{0,3}	6.24(-13)	0.76	0.21	7.48(-13)	0.53	0.26	2.76(-12)	0.41	0.50	4.95(-12)	0.43	0.55
3 _{2,1} → 3 _{1,2}	7.88(-12)	0.60	0.34	1.49(-11)	0.67	0.49	5.17(-11)	0.91	0.75	8.08(-11)	1.11	0.90
4 _{1,4} → 1 _{0,1}	2.92(-12)	1.93	0.59	3.14(-12)	1.08	0.64	7.97(-12)	1.22	1.21	1.31(-11)	1.43	1.84
4 _{1,4} → 1 _{1,0}	2.56(-13)	0.22	0.29	4.30(-13)	0.16	0.36	2.48(-12)	0.22	0.53	5.24(-12)	0.32	0.62
4 _{1,4} → 2 _{1,2}	1.00(-12)	1.99	0.33	1.43(-12)	1.17	0.35	5.55(-12)	1.43	1.05	1.05(-11)	1.81	1.84
4 _{1,4} → 2 _{2,1}	9.88(-13)	0.50	0.52	1.39(-12)	0.43	0.61	3.92(-12)	0.49	0.93	6.30(-12)	0.56	1.11
4 _{1,4} → 3 _{0,3}	2.00(-11)	1.32	0.40	2.24(-11)	0.91	0.46	5.41(-11)	0.94	0.72	8.01(-11)	1.10	0.88
4 _{1,4} → 3 _{1,2}	1.56(-13)	0.16	0.08	4.46(-13)	0.29	0.18	9.40(-13)	0.20	0.34	2.01(-12)	0.27	0.46
4 _{1,4} → 3 _{2,1}	7.27(-13)	0.78	0.26	1.23(-12)	0.43	0.31	4.88(-12)	0.65	0.61	8.47(-12)	0.92	0.90
3 _{3,0} → 1 _{0,1}	3.03(-13)	61.35	5.14	4.20(-13)	17.93	4.59	2.15(-12)	4.01	6.86	4.86(-12)	3.80	5.48
3 _{3,0} → 1 _{1,0}	2.08(-12)	7.12	1.82	2.64(-12)	2.59	1.91	8.23(-12)	1.16	1.67	1.34(-11)	1.04	1.49
3 _{3,0} → 2 _{1,2}	8.40(-13)	2.66	0.86	1.06(-12)	1.13	0.85	3.44(-12)	0.67	0.90	5.61(-12)	0.66	0.89
3 _{3,0} → 2 _{2,1}	2.71(-11)	4.51	0.80	2.92(-11)	2.04	0.76	5.89(-11)	1.28	0.88	8.29(-11)	1.35	1.01
3 _{3,0} → 3 _{0,3}	4.90(-13)	1.08	0.46	4.70(-13)	0.47	0.39	1.29(-12)	0.24	0.54	2.97(-12)	0.31	0.79
3 _{3,0} → 3 _{1,2}	5.68(-13)	0.66	0.31	6.31(-13)	0.34	0.41	4.16(-12)	0.53	1.10	9.61(-12)	0.82	1.49
3 _{3,0} → 3 _{2,1}	8.63(-12)	0.73	0.38	1.07(-11)	0.63	0.44	3.05(-11)	0.94	0.78	4.82(-11)	1.25	1.04
3 _{3,0} → 4 _{1,4}	5.47(-13)	0.76	0.41	3.98(-13)	0.21	0.40	2.23(-12)	0.23	0.74	5.30(-12)	0.36	0.95

Baulch, D. L., Cobos, C. J., Cox, R. A., et al. 1992, *J. Phys. Chem. Ref. Data*, 21, 411
Caselli, P., Keto, E., Bergin, E. A., et al. 2012, *ApJL*, 759, L37
Caselli, P., Keto, E., Pagani, L., et al. 2010, *A&A*, 521, L29
Cernicharo, J., Goicoechea, J. R., Daniel, F., et al. 2006, *ApJL*, 649, L33
Cernicharo, J., & Crovisier, J. 2005, *Space Sci. Rev.*, 119, 29
Cernicharo, J., Pardo, J. R., González-Alfonso, E., et al. 1999, *ApJL*, 520, L131
Cernicharo, J., Gonzalez-Alfonso, E., Alcolea, J., Bachiller, R., & John, D. 1994, *ApJL*, 432, L59
Chu, S.-I., & Dalgarno, A. 1975, *Royal Society of London Proceedings Series A*, 342, 191
Dagdigian, P. J., & Alexander, M. H. 2013, *J. Chem. Phys.*, 139, 194309

Daniel, F., Dubernet, M.-L., Pacaud, F., & Grosjean, A. 2010, *A&A*, 517, A13
Daniel, F., Dubernet, M.-L., & Grosjean, A. 2011, *A&A*, 536, A76
Daniel, F., & Cernicharo, J. 2013, *A&A*, 553, A70
Decin, L., Agúndez, M., Barlow, M. J., et al. 2010, *Nature*, 467, 64
van Dishoeck, E. F., Kristensen, L. E., Benz, A. O., et al. 2011, *PASP*, 123, 138
van Dishoeck, E. F., Herbst, E., & Neufeld, D. A. 2013, *Chemical Reviews*, 113, 9043
Dubernet, M.-L., & Grosjean, A. 2002, *A&A*, 390, 793
Dubernet, M.-L., Daniel, F., Grosjean, A., et al. 2006, *A&A*, 460, 323
Dubernet, M.-L., Daniel, F., Grosjean, A., & Lin, C. Y. 2009, *A&A*, 497, 911

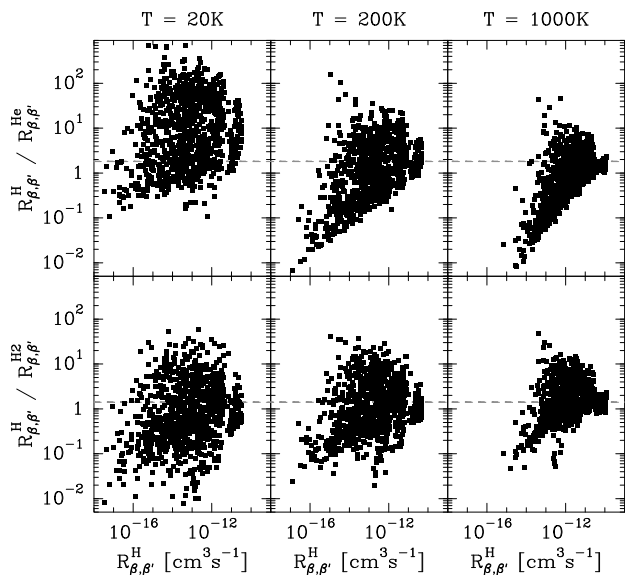


Figure 1. Ratios of the He ($R_{\beta,\beta'}^{\text{He}}$ from Green et al. 1993) and H_2 ($R_{\beta,\beta'}^{\text{H}_2}$ from Dubernet et al. 2009) collisional rate coefficients with the o- H_2O rates calculated with H ($R_{\beta,\beta'}^{\text{H}}$) as a collider. These values are given as a function of the magnitude of $R_{\beta,\beta'}^{\text{H}}$ and for temperatures of 20K (first column) 200K (second column) and 1000K (third column).

Schöier, F. L., van der Tak, F. F. S., van Dishoeck, E. F., & Black, J. H. 2005, *A&A*, 432, 369
 Stoecklin, T., Voronin, A., & Rayez, J. C. 2004, *Chemical Physics*, 298, 175
 Stoecklin, T., & Voronin, A. 2007, *Chemical Physics*, 331, 385
 Shepler, B. C., Yang, B. H., Dhillip Kumar, T. J., et al. 2007, *A&A*, 475, L15
 Valiron, P., Wernli, M., Faure, A., et al. 2008, *J. Chem. Phys.*, 129, 134306
 Walker, K. M., Yang, B. H., Stancil, P. C., Balakrishnan, N., & Forrey, R. C. 2014, *ApJ*, 790, 96
 Wrathmall, S. A., & Flower, D. R. 2006, *Journal of Physics B Atomic Molecular Physics*, 39, L249
 Yang, B., Stancil, P. C., Balakrishnan, N., Forrey, R. C., & Bowman, J. M. 2013, *ApJ*, 771, 49

This paper has been typeset from a $\text{T}_\text{E}\text{X}/\text{L}_\text{A}\text{T}_\text{E}\text{X}$ file prepared by the author.

Dubernet, M.-L., Alexander, M. H., Ba, Y. A., et al. 2013, *A&A*, 553, A50
 Faure, A., Valiron, P., Wernli, M., et al. 2005, *J. Chem. Phys.*, 122, 221102
 Faure, A., & Josselin, E. 2008, *A&A*, 492, 257
 Faure, A., Gorfinkiel, J. D., & Tennyson, J. 2004, *MNRAS*, 347, 323
 Flower, D. R., Le Bourlot, J., Pineau des Forêts, G., & Cabrit, S. 2003, *MNRAS*, 341, 70
 Flower, D. R., & Pineau Des Forêts, G. 2010, *MNRAS*, 406, 1745
 Flower, D. R., & Roueff, E. 1998, *Journal of Physics B Atomic Molecular Physics*, 31, L955
 Flower, D. R., & Roueff, E. 1999, *MNRAS*, 309, 833
 Forrey, R. C., Balakrishnan, N., Dalgarno, A., & Lepp, S. 1997, *ApJ*, 489, 1000
 Fu, B., & Zhang, D. H. 2013, *JCP*, 138, 184308
 González-Alfonso, E., Smith, H. A., Fischer, J., & Cernicharo, J. 2004, *ApJ*, 613, 247
 González-Alfonso, E., & Cernicharo, J. 1999, *ApJ*, 525, 845
 Green, S., & Thaddeus, P. 1976, *ApJ*, 205, 766
 Green, S., Maluendes, S., & McLean, A. D. 1993, *ApJS*, 85, 181
 Grosjean, A., Dubernet, M.-L., & Ceccarelli, C. 2003, *A&A*, 408, 1197
 Hollenbach, D., Elitzur, M., & McKee, C. F. 2013, *ApJ*, 773, 70
 Jiang, B., Xie, D., & Guo, H. 2011, *JCP*, 135, 084112
 Lique, F., Honvault, P., & Faure, A. 2012, *J. Chem. Phys.*, 137, 154303
 Lique, F., & Faure, A. 2012, *J. Chem. Phys.*, 136, 031101
 Neufeld, D. A., Gusdorf, A., Güsten, R., et al. 2014, *ApJ*, 781, 102
 Kyrö, E. 1981, *Journal of Molecular Spectroscopy*, 88, 167
 Nesterenok, A. V., & Varshalovich, D. A. 2014, arXiv:1407.3135
 Patkowski, K., Korona, T., Moszynski, R., Jeziorski, B., Szalewicz, K. 2014, *J. Mol. Struct. (Theochem)*, 591, 231
 Roueff, E., & Flower, D. R. 1999, *MNRAS*, 305, 353